Biomedicine & Pharmacotherapy 169 (2023) 115880

Contents lists available at ScienceDirect

Biomedicine & Pharmacotherapy

journal homepage: www.elsevier.com/locate/biopha

20(S)-ginsenoside Rh2 inhibits angiotensin-2 mediated cardiac remodeling and inflammation associated with suppression of the JNK/AP-1 pathway

Tianxiang Yu [a,b], Jiachen Xu [b], Qinyan Wang [b], Xue Han [a,b], Yu Tu [a], Yi Wang [b], Wu Luo [b,d], Mengyang Wang [a,c,*], Guang Liang [a,b,*]

[a] Department of Pharmacy and Institute of Inflammation, Zhejiang Provincial People's Hospital, Affiliated People's Hospital, Hangzhou Medical College, Hangzhou, Zhejiang 310014, China
[b] Chemical Biology Research Center, School of Pharmaceutical Sciences, Wenzhou Medical University, Wenzhou, Zhejiang 325035, China
[c] Department of Pharmacology, College of Pharmacy, Beihua University, Jilin, Jilin132013, China
[d] Department of Cardiology, the First Affiliated Hospital of Wenzhou Medical University, Wenzhou, Zhejiang 325035, China

ARTICLE INFO

Keywords:
20(S)-ginsenoside Rh2
Angiotensin II
C-Jun N-terminal kinase
Inflammation
Hypertensive heart failure

ABSTRACT

Background: Enhanced levels of angiotensin-2 (Ang-II) causes hypertensive heart failure (HHF) through non-hemodynamical and hemodynamical alterations. 20(S)-ginsenoside Rh2 (20(S)-Rh2) is a natural ginseng compound with numerous cardiovascular benefits. This investigation elucidates the influence of 20(S)-Rh2 on Ang-II-induced heart failure and cardiac alterations.
Methods: Ang-II was administered in C57BL/6 mice for 4 weeks to induce HHF. In the last 2 weeks of treatment, 20(S)-Rh2 was orally administered in mice to assess the potential 20(S)-Rh2 mechanism. Subsequently, RNA sequencing was carried out.
Results: It was indicated that 20(S)-Rh2 suppresses myocardial fibrosis, hypertrophy, and inflammation, thereby inhibiting cardiac disruption in Ang-II-challenged mice without affecting blood pressure. According to the RNA sequencing data, this cardio-protective effect was linked with the (JNK)/AP 1 pathway. 20(S)-Rh2 alleviated heart tissue and cardiomyocytes inflammation by inhibiting the Ang-II-mediated JNK/AP-1 pathway. Within cardiomyocytes, JNK or AP-1 absence abolished the anti-inflammatory effects of 20(S)-Rh2.
Conclusion: This study investigation indicated that 20(S)-Rh2 prevents cardiovascular dysfunction induced by Ang-II induced by decreasing JNK-regulated inflammatory responses, providing evidence for its use as an efficient regimen for HHF.

1. Introduction

It has been identified that > 30% of adults have hypertension, significantly contributing to the prevalence of cardiovascular diseases (CVD), including heart failure, myocardial infarction, and stroke [1]. Increased level of angiotensin-2 (Ang-II) stimulates the local renin-angiotensin system (RAS), causing heart dysregulation, such as hypertrophy and cardiac remodeling [2]. Ang-II is a cytokine with different activities and induces inflammation and oxidative stress, damaging the heart and blood vessels [3]. Ang-II promotes the inflammatory phenotype of cardiomyocytes, which is associated with cardiac fibrosis and remodeling [4]. Since, clinically, RAS inhibitors targeting hypertension cannot completely reverse the cardiac dysfunction and remodeling [5], pursuing drugs against Ang-II effects, like Ang-II-mediated chronic inflammation, is beneficial from a non-hemodynamic perspective.

For centuries natural medicines have been utilized to prevent and cure diseases. In modern medicine, Traditional Chinese medicine (TCM) is considered the safest regimen. For instance, ginseng has been utilized for decades as a natural remedy. Rh2 is a hydrolyzed ginsenosides product and the principal active pharmacological component in ginseng. Ginsenosides are a type of natural-product steroid glycosides that broadly influence the cardiovascular, central nervous, and immunological systems [6–9]. Rh2 has indicated substantial anti-inflammatory, antiallergy, anticancer, hypoxia-resistant, immune-boosting, and CVD preventive activities [10–13]. It is purer, has a faster drug metabolism

* Corresponding authors at: Department of Pharmacy and Institute of Inflammation, Zhejiang Provincial People's Hospital, Affiliated People's Hospital, Hangzhou Medical College, Hangzhou, Zhejiang 310014, China.
E-mail addresses: 15643584357@163.com (M. Wang), wzmcliangguang@163.com (G. Liang).

https://doi.org/10.1016/j.biopha.2023.115880
Received 29 August 2023; Received in revised form 8 November 2023; Accepted 9 November 2023
Available online 11 November 2023

rate than ginsenoside [14], and effectively lowers cardiac fibrosis in various CVDs [10]. Based on its distinct spatial structures in Rh2, C20 can be divided into two stereoisomerism forms namely 20(S)-ginsenoside Rh2 (20(S)-Rh2) and 20(R)-ginsenoside Rh2 (Fig. 1A) [12]. 20(S)-Rh2 suppresses doxorubicin-stimulated cardiac enzymes released into the serum and reduces pathological changes by restoring reduced antioxidant biomolecules and accumulated malondialdehyde in heart tissues [15]. However, the efficiency of 20(S)-Rh2 against hypertensive heart failure (HHF) is still undetermined.

This investigation elucidates the cardio-protective properties of 20(S)-Rh2 against hypertension. 20(S)-Rh2′s ability to inhibit c-Jun N-terminal kinase (JNK) together with produced activator protein 1 (AP-1) blocks Ang-II-mediated cardiac hypertrophy, and inflammation, together with fibrosis at multiple levels. It was revealed that 20(S)-Rh2 could serve as an efficient novel HHF drug.

2. Materials and methods

2.1. Chemicals

Supplementary Table S1 enlists all the reagents and antibodies utilized.

2.2. Cell culture

To isolate neonatal rat ventricular myocytes (NRVMs), neonatal rats were sacrificed and then heart tissues were removed, washed in PBS, and digested using a mixture of pancreatin and collagenase. Fibroblasts were removed by differential adherence culture. Fibroblasts were cultured in Dulbecco's modified Eagle medium (DMEM, cat no.11995040, Gibco™; Germany) containing 4.5 g/L glucose and 10% fetal bovine serum (Gibco; cat no.14160063, Germany). Myocytes were also cultured in the same media with the addition of 5-BrdU (HY-15910, Med Chem Express, New Jersey, USA). After 48 h of culture, NRVMs exhibited regular pulsation and were used for experiments. For some experiments, a rat cardiomyocyte-like cell line H9c2 obtained from the Shanghai Institute of Biochemistry and Cell Biology, was used. These cells were propagated at 37 °C within DMEM, augmented through 1% penicillin/streptomycin and 10% fetal bovine serum in 5% CO_2 incubator (Invitrogen; CA, USA).

2.3. Animal experiment

Animal Center of Wenzhou Medical University provided C57BL/6 (n = 24, age = 6 w, weight = 16–17 g) mice. The in vivo protocols were authorized by the University's Animal Policy and Welfare Committee (Approval # wydw2021–1031). The recommendations from the National Institutes of Health (USA) were complied. Mice were acclimatized to the environment 2 weeks prior to in vivo analyses in a standard laboratory with a 12-hour light cycle and standard chow.

For 4 weeks, Ang-II was infused in mice to induce hypertensive cardiac damage using a micro-osmotic pump (cat # Alzet™ MODEL 1004, USA) [16] at 1 ng/kg/min rate after implantation in the mice back. Post-pump insertion, mice were given neomycin (1 g/L) augmented water to avoid wound infection. Weekly, mice's systolic blood pressure (SBP) was assessed via telemetric blood pressure apparatus having tail cuff (BP-2010A, Softron Biotech™, Japan) [17]. 2 weeks after starting Ang-II treatment, 20(S)-Rh2 dissolved 0.5% CMC-Na was injected in mice intragastrically. 20(S)-Rh2 dosages of 20 and 50 mg/kg/d were opted for after a literature review [18,19]. Using randomization, mice were categorized into 4 groups (n = 6): 1) CON = non-treated mice who received 0.5% CMC-Na vehicle solution, 2) Ang-II = mice who received Ang-II and 0.5% CMC-Na vehicle solution, 3) Ang-II + 20 mg/kg 20(S)-Rh2 = mice who received Ang-II and 20(S)-Rh2 (20 mg/kg) daily, and 4) Ang-II + 50 mg/kg 20(S)-Rh2 = mice who received Ang-II and 20(S)-Rh2 (50 mg/kg) daily.

All mice survived the treatments and were euthanized using sodium pentobarbital after the completion of the experiment to collect cardiac tissues and blood. The total body mass, tibia length, and heart weight were assessed. Changes in serum ANP, CK-MB, and Ang II indicators of mice were evaluated using commercial kits. The tissue specimens were liquid nitrogen-frozen immediately to assess protein / gene expression-profiles, whereas they were preserved in 4% paraformaldehyde (PFA) for histology-based assessments.

2.4. Cardiac function assays

One day before euthanization, transthoracic echocardiography was carried out via SONOS 5500™ ultrasonography having a 15-MHz linear array ultrasound transducer (Philips™, Netherlands) to noninvasively measure systolic and diastolic heart function. Isoflurane was used for the sedation.

2.5. WGA-FITC staining

For immunofluorescence staining, for 10 min the frozen cardiac tissue specimens were rendered permeable by 0.1% Triton X-100, sliced (5 μm thick), occluded by BSA (5%; thirty minutes), stained with WGA-FITC (1:200) at 37 °C for 30 min, and imaged at 40 × magnification through fluorescence microscopy (Nikon™, Japan).

2.6. Cardiac histological assessment

Paraffin-immersed heart tissues were sliced (5 μm thick) and dyed with Masson's trichrome, H&E, together with Sirius Red to assess collagen levels at 200 × magnification via a light microscope (Nikon™, Japan). Image J® (NIH) software performed collagen quantification by the single-blind method.

2.7. Rhodamine phalloidin staining

Treated NRVMs were preserved within 4% PFA, rendered permeable by Triton® X-100 (0.1%), dyed for 30 min with 50 ng/mL of rhodamine-conjugated phalloidin to assess hypertrophic cellular changes, stained nuclei with DAPI at ambient temperature and imaged with the help of an epifluorescence microscopy (400 × magnification; Nikon™, Japan).

2.8. Cellular viability analysis

H9c2 cells (3000/well) were propagated overnight within 96-well plates, treated with different 20(S)-Rh2 concentrations (0.1, 0.5, 1, 2.5, 5, 10, 20, 40, and 80 μM) for 24 h. DMSO was given to control cells instead of 20(S)-Rh2. After incubating, methyl thiazolyl tetrazolium (MTT) was inoculated per well (four hours) before DMSO addition and optical density assessment via SpectraMax® M5 microplate reader (Molecular Devices™, USA) (570 nm). Cellular viability was compared with the controls.

2.9. RNA transcriptome sequencing

Whole mouse heart tissue RNA was acquired via Trizol (Invitrogen, CA, USA) reagent per kit's guide, quantified, and assessed for purity by NanoDrop ND-100 (DE). RNAs' integrity was elucidated via a Bioanalyzer 2100 (Agilent, CA) and then confirmed on denatured agarose gel by electrophoresis assay. With the help of Dynabeads® Oligo (dT) 25–61005 (Thermo-Fisher, USA), poly (A) RNA was separated from whole RNA (1 μg), which was then fragmented by magnesium RNA Fragmentation Module (NEB, cat. e6150, MA), and cDNA-converted through SuperScriptTM II (Invitrogen™, cat. 1896649, USA). Sequencing was completed through Illumina™ NovaseqTM 6000 per kit's guide. The transcripts were quantified after the generation of the whole transcriptome. Differential expression mRNAs were assessed as follows: 2 > fold change < 0.5 and $P < 0.05$.

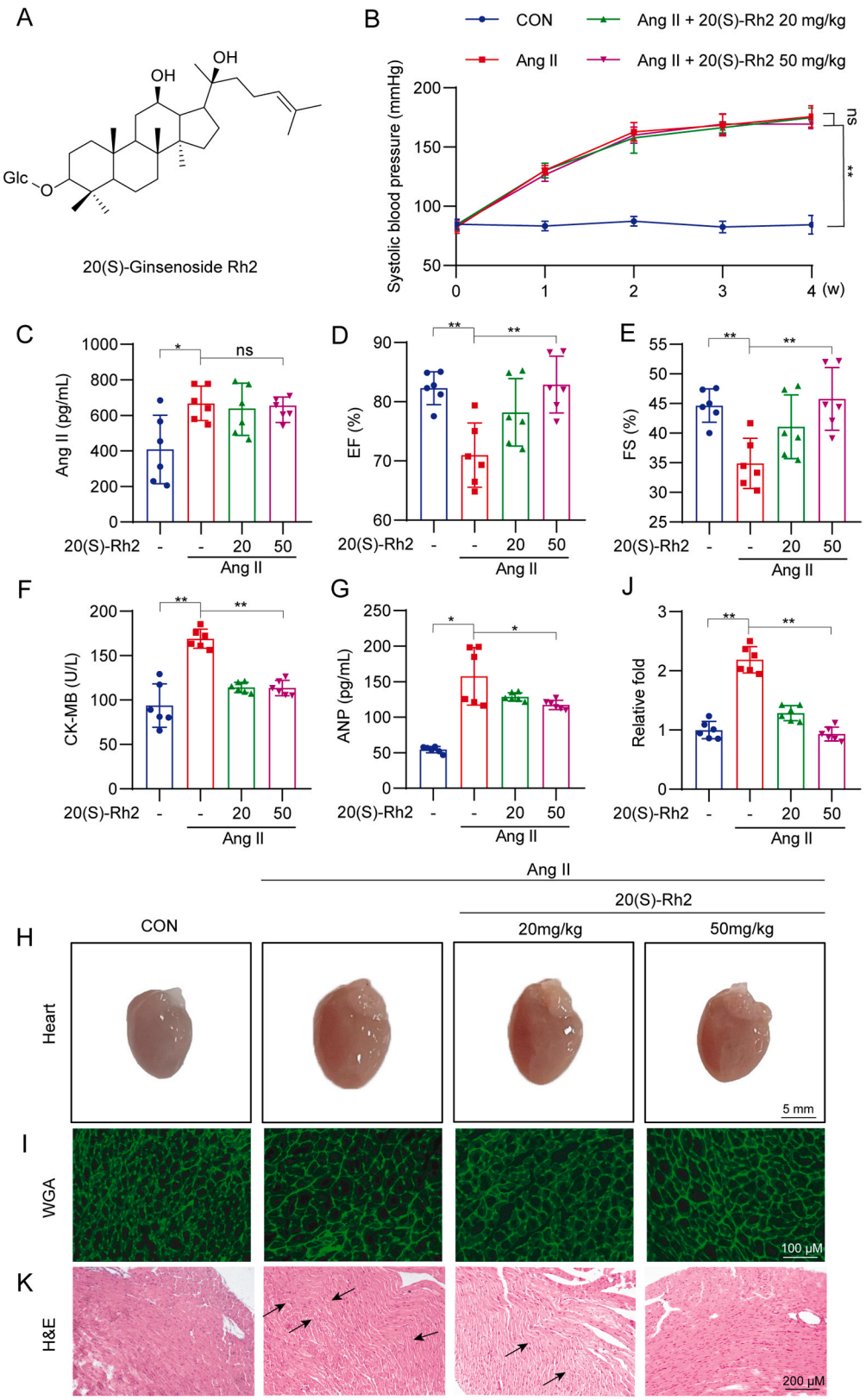

Fig. 1. 20(S)-Rh2 inhibits cardiac dysfunction and remodeling induced by Ang-II infusion in mice. (A) Chemical structure for 20(S)-Rh2. (B) Weekly SBP assessment. (C) Mice serum Ang-II levels were elucidated via ELISA. (D–E) Mice EF and FS were elucidated using an ultrasonic scanning image system. (F–G) Mice serum CK-MB and ANP levels were assessed by biochemical and ELISA kits. (H) Representative heart images on a white background. (I) Heart tissues' representative WGA staining images (scale bar = 100 μm). (J) Quantitative assessment of the myocyte area. At least 100 cells (4 samples/group) were calculated from various visual fields. (K) Heart tissues' representative H&E staining images (scale bar = 200 μm). The black arrows depict myocardial fiber arrangement disorder. Datasets reflected Mean ± SEM; n = 6; ns = not significant; * = $p < 0.05$, ** = $p < 0.01$, two-tailed Student's *t*-test.

2.10. Real-time qPCR (RT-qPCR)

Whole cellular and tissue RNA was acquired utilizing Trizol, transcribed reversely with PrimeScript® RT (DRR037A, TakaraBio™, Japan), and then used for qRT-PCR (Bio-Rad; CA, USA) through CFX96® Touch Real-Time PCR Detection System, TB Green® Premix Ex Taq™ II (RR820B, Takara Bio™, Japan) together with specific primers. β-actin was set for normalizing gene expression levels. Supplementary Table S2 enlists details for primers used.

2.11. Western blot assay

Cellular and tissue lysates were exposed onto 10% SDS-PAGE, transplanted on the PVDF membranes, and blocked. 1.5 h in Tris-buffered saline with non-fat milk (5%) and Tween20 (0.05%), labeled with concerned primary antibodies, then using secondary antibodies tagged with horseradish peroxidase, consequently observed after using chemiluminescence reagent (Bio-Rad™, USA). Image J version 1.38e was utilized for analysis; densitometric values were standardized with their specific controls.

2.12. Statistical measurements

The statistical measurements were carried out via GraphPad Prism® v8.0 (GraphPad™, USA) software and included a one-way analysis of variance (ANOVA) and Bonferroni correction for multiple comparisons. Datasets reflected mean ± SEM, and $P < 0.05$ was termed essential.

3. Results

3.1. 20(S)-Rh2 inhibits cardiac dysfunction and remodeling induced by Ang-II infusion in mice

To assess if 20(S)-Rh2 inhibits in vivo cardiac damage induced by Ang-II, mice SBP was enhanced, and it was indicated that 20(S)-Rh2 treatment had no effect on blood pressure (Fig. 1B). Furthermore, Ang-II induction increased serum Ang-II concentrations, and 20(S)-Rh2 did not influence this elevation (Fig. 1C). These data indicate that 20 (S)-Rh2 does not have the function of lowering blood pressure. Moreover, noninvasive echocardiography indicated that 20(S)-Rh2 dose-dependently alleviated Ang-II stimulated heart dysfunction, as indicated by the reversal of ejection fraction (EF) and fractional shortening (FS) percentages within 20(S)-Rh2-injected hypertensive mice (Fig. 1D-E, Supplementary Fig. S1, and Table 1). Additionally, 20(S)-Rh2 dose-dependently decreased serum ANP and CKMB concentrations in Ang-II-challenged mice (Fig. 1F-G). Next, the influence of 20(S)-Rh2 on hearts' morphological deterioration was assessed. Gross analysis and WGA staining indicated hypertrophic changes in the Ang-II-challenged mice's hearts, whereas 20(S)-Rh2 substantially reversed this effect (Fig. 1H-J). The ratios of heart weight/tibia length and heart weight/body weight also confirm these results (Table 1). Through H&E staining, it was also found that 20 (S)-Rh2 treatment significantly alleviated Ang II induced histological changes in mice hearts (Fig. 1K). Altogether, it was suggested that 20(S)-Rh2 is an effective shield protecting the hearts from the functional impairment and hypertrophy typically caused by Ang-II.

3.2. 20(S)-Rh2 protects mice against Ang-II-induced cardiac inflammation and fibrosis

Upon heart fibrosis analysis by Sirius Red/Masson's trichrome stain-steps, 20(S)-Rh2 was substantially alleviated Ang-II-induced cardiac fibrosis (Fig. 2A-B, Supplementary Fig. S2A-B). Upregulated proteomic/transcriptomic levels for TGF-β1, β-MyHC, and COL-1 validated the presence of cardiac fibrosis and hypertrophy in Ang-II mice. These alterations were markedly reversed by 20(S)-Rh2 treatment in a dose-dependent pattern (Fig. 2C-E). Additionally, the inflammatory genes mRNA levels, such as interleukin (*Il1β*, *Il6*), together with tumor necrosis factor-α (*Tnfα*), were notably increased in the Ang-II mice's hearts, almost completely reversed by the 20(S)-Rh2 regimen (Fig. 2F). We also measured the mRNA level of *F4/80* in mouse hearts. As shown in Supplementary Fig. S2C, the mRNA level of *F4/80* was significantly increased in the hearts of Ang II-infusion mice, while this increase was reversed by 20(S)-Rh2 treatment, indicating that 20(S)-Rh2 reduces cardiac macrophage infiltration in Ang II-challenged mice.

Table 1
Biometric and Echocardiographic Measurements in Experimental Mice.

	CON	Continuous Ang II Pump Infusion		
			20 (S)-Rh2 (20 mg/kg)	20 (S)-Rh2 (50 mg/kg)
	n = 6	n = 6	n = 6	n = 6
EF, %	82.30 ± 2.77	70.99 ± 5.43**	78.21 ± 5.7##	82.89 ± 4.77##
FS, %	44.65 ± 2.81	34.88 ± 4.24**	41.08 ± 5.39##	45.78 ± 5.29##
LVIDd, mm	2.1 ± 0.26	3 ± 0.49**	2.77 ± 0.50	2.48 ± 0.22#
IVSD, mm	0.63 ± 0.08	0.75 ± 0.05 *	0.67 ± 0.05#	0.65 ± 0.05#
PWD, mm	0.62 ± 0.08	0.74 ± 0.05 *	0.65 ± 0.05#	0.67 ± 0.05#
E wave, m/s	0.676 ± 0.06	0.60 ± 0.09	0.57 ± 0.07	0.68 ± 0.06
Tei Index	0.59 ± 0.06	0.79 ± 0.13**	0.75 ± 0.14	0.64 ± 0.08#
IRT, ms	12.83 ± 1.60	16.83 ± 1.33**	15.83 ± 1.60	14.83 ± 0.98#
HW/BW, mg/g	5.51 ± 0.26	6.17 ± 0.45 *	5.52 ± 0.65	5.07 ± 0.43##
HW/TL, mg/mm	6.11 ± 0.47	8.37 ± 0.52**	6.47 ± 0.97##	6.39 ± 0.48##

Transthoracic echocardiography was performed on mice at the end of the animal study. Ang II, angiotensin II; BW, body weight; CON, control; EF, ejection fraction; E wave, peak mitral E velocity; FS, fractional shortening; HW, heart weight; IRT, isovolumic relaxation time; IVSD, diastole interventricular septal thickness; LVIDd, diastole left ventricle internal dimension; PWD, diastole posterior wall thickness; Tei index, a myocardial performance index designed by Dr. Chuwa Tei. Data presented as mean ± SEM.
* $p < 0.05$,
** $p < 0.01$ compared with CON group;
# $p < 0.05$,
$p < 0.01$ compared with Ang II Pump.

3.3. The 20(S)-Rh2 cardioprotective effect is linked to JNK/AP-1 inhibition

Cardiac tissue RNA was sequenced to assess the possible 20(S)-Rh2 heart-protecting mechanism. 203 genes (133 upregulated and 70 downregulated) in the Ang-II group were markedly different from the control mice (Fig. 3A). Furthermore, in the 20(S)-Rh2 +Ang-II group, 131 genes (46 upregulated and 85 downregulated) were different from the control mice (Fig. 3B). It was revealed that 20(S)-Rh2 controlled 20 genes under Ang-II stress (Fig. 3C), their expression analysis via BioPlanet 2019 indicated the association for JNK/MAPK pathway (Fig. 3D). MAPK is critically linked with inflammation [20]. JNK is a MAPK family member and is stimulated by different stressors, inflammatory cytokines, and growth mediators. JNK activation has been observed to cause HHF [21]. Here, western blot analysis revealed an increase in the phosphorylation of JNK in the Ang-II mice hearts. At the same time, which was decreased by 20(S)-Rh2 therapy (Fig. 3E-F). AP-1 is a nuclear transcription activator composed of c-Fos and c-Jun [22]. Generally, the nuclear translocation of c-Jun has been widely used to indicate the activation of AP-1 transcriptional factor [23,24]. We examined the nuclear translocation of c-Jun to characterize if 20(S)-Rh2 had any impact

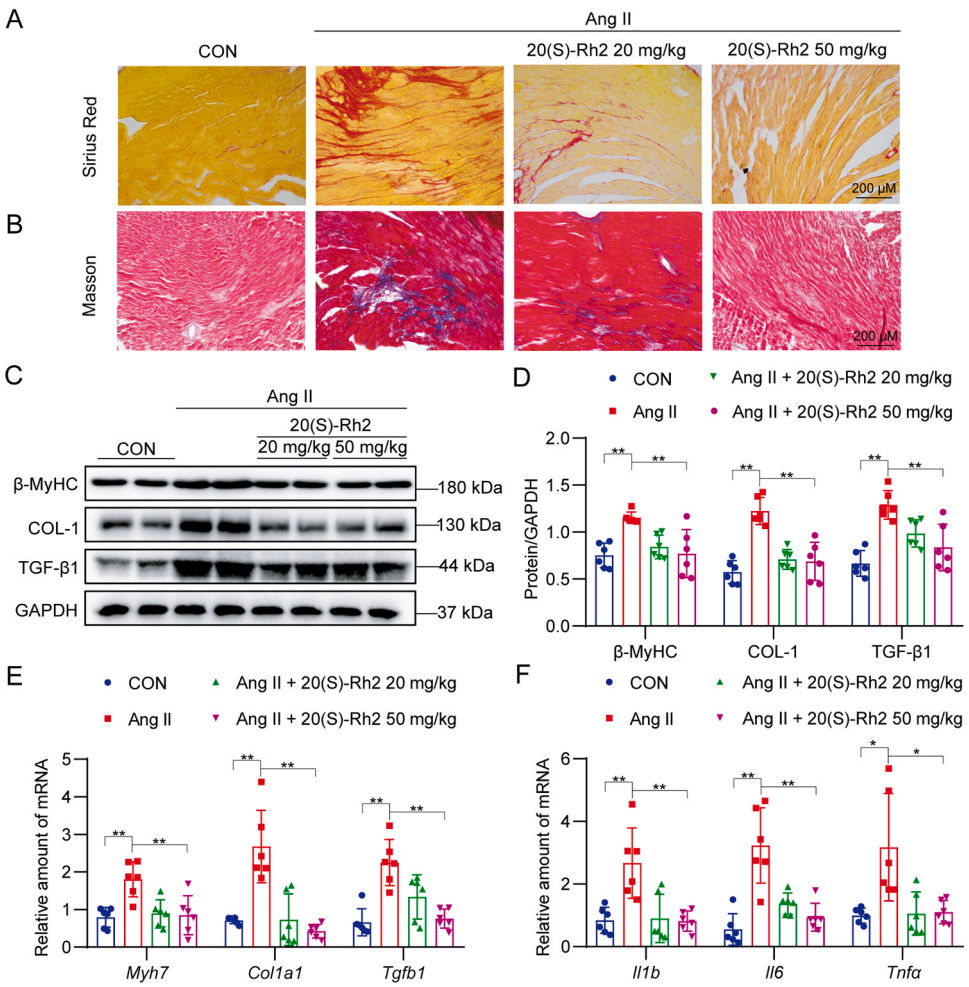

Fig. 2. 20(S)-Rh2 protects mice against Ang-II-induced cardiac inflammation and fibrosis. (A) Hearts' Sirius Red staining representative micrographs. (B) Masson trichrome stained representative micrographs (scale bar = 200 μm). (C) Western blot data of COL-1, β-MyHC, and TGF-β1 in mouse heart tissues. GAPDH was utilized as endogenous control. **(D)** Proteins' quantitative blot intensity data was assessed via ImageJ in plane C. **(E-F)** The mRNA levels of *Col1a*, *myh7*, *Tgfb1*, *Il1b*, *Tnfα*, and *Il6* in mouse heart tissues were assessed by RT-qPCR. Datasets reflected Mean ± SEM; n = 6; * = $p < 0.05$, ** = $p < 0.01$, two-tailed Student's *t*-test.

on Ang-II-mediated AP-1 activation. Ang-II induction enhances the nuclear translocation of c-Jun in the wild-type mice hearts, which was abolished after 20(S)-Rh2 treatment dose-dependently (Fig. 3G-H).

3.4. 20(S)-Rh2 inhibits Ang-II-mediated fibrosis, inflammation, and hypertrophy in NRVMs and cardiac fibroblasts

To evaluate if 20(S)-Rh2 cardio-protection occurs by directly targeting cardiomyocytes, MTT test was carried out, which indicated that 0.1–20 μM 20(S)-Rh2 concentrations did not harm H9c2 cultures (Supplementary Fig. S3). 20(S)-Rh2 inhibited Ang-II-induced enhanced protein and mRNA levels of β-MyHC, COL-1, and TGF-β1 dose-dependently, as assessed by RT-qPCR and western blotting in NRVMs and fibroblasts, respectively (Fig. 4A-B, Supplementary Fig. S4A-D). Rhodamine-phalloidin labeling revealed 20(S)-Rh2 blocks Ang-II-mediated hypertrophy in NRVMs (Fig. 4C-D). Moreover, according to the RT-qPCR, Ang-II increased the inflammatory genes *Il1b*, *Tnfa,* and *Il6* mRNA levels, which was reversed by 20(S)-Rh2 (Fig. 4E). These data suggest that 20(S)-Rh2 suppresses Ang-II-mediated hypertrophy, inflammation, and fibrosis in cardiomyocytes and fibroblasts, respectively.

3.5. 20(S)-Rh2 protects cardiomyocytes by inhibiting JNK/AP-1 activation

To assess if the in vivo 20(S)-Rh2s' cardio-protective effects are linked with JNK suppression, immunoblot analysis was carried out, which indicated increased JNK phosphorylation in Ang-II-treated NRVMs. However, 20(S)-Rh2 therapy significantly alleviated p-JNK levels (Fig. 5A-B). As shown in Fig. 5C-H, JNK inhibitors reduced the Ang-II-mediated mRNA levels of pro-hypertrophic gene (*Myh7*), pro-inflammatory genes (*Il6, Tnfα, and Il1b*) in NRVMs, and pro-fibrotic genes (*Tgfb1* and *Col1a1*) in fibroblasts. SP600125's inhibition for JNK alleviated 20(S)-Rh2s' intrinsic preventive effects on Ang-II-mediated transcriptomic expression-profile for above genes (Fig. 5C-H). Furthermore, to confirm if the nuclear translocation of AP-1 was also blocked after JNK inhibition, nuclear c-Jun levels were assessed (Fig. 5I-J). Altogether, 20(S)-Rh2 inhibits JNK/AP-1 activation to prevent Ang-II-induced cardiomyocyte damage.

4. Discussion

The investigation revealed that 20(S)-Rh2 inhibits HHF by blocking JNK/AP-1-modulated cardiac inflammation in Ang-II induced mice; 20 (S)-Rh2 reduced heart hypertrophy, fibrosis, and cardiac dysfunction; moreover, it effectively decreased Ang-II's triggered JNK/AP-1 activation in an in vivo and in vitro protocols. The Ang-II caused pathological

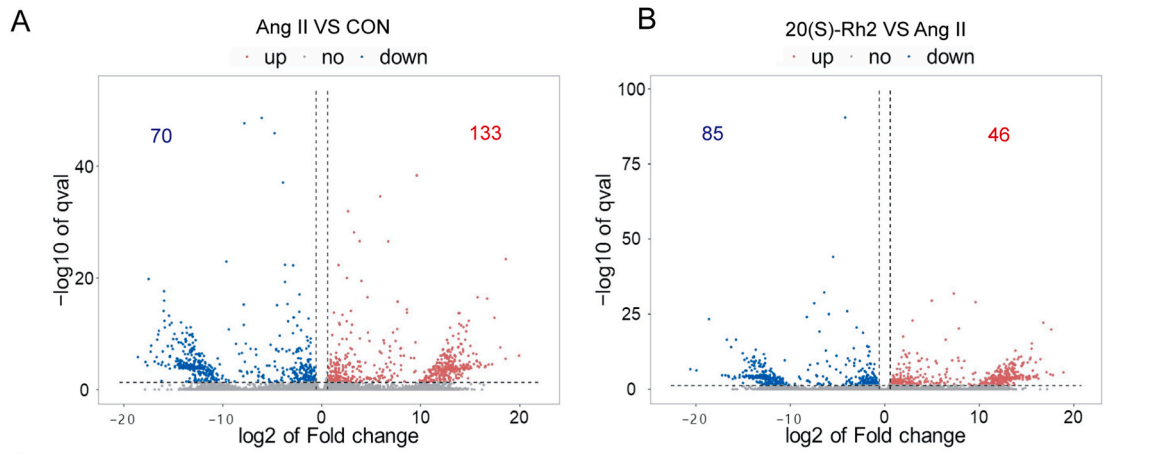

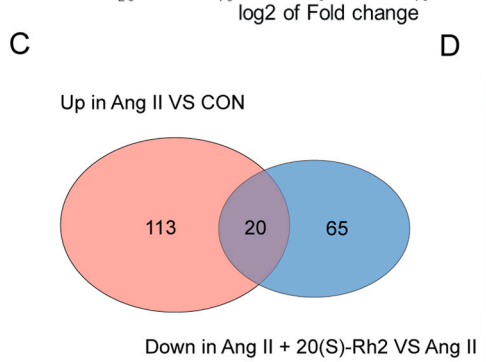

D

BioPlanet 2019			
Index	**Name**	**P-value**	**Odds Ratio**
31	HNF3B pathway	0.04407	23.85
32	Syndecan 1 pathway	0.04503	23.32
33	Actions of nitric oxide in the heart	0.04599	22.81
34	Agrin in postsynaptic differentiation	0.04599	22.81
35	Amino acid and oligopeptide SLC transproters	0.04790	21.86
36	Muscle contraction	0.04790	21.86
37	Type 2 diabetes mellitus	0.04885	21.41
38	JNK/MAPK pathway	0.05171	20.17
39	starch and sucrose metabolism	0.05171	20.17
40	Caspase cascade in apoptosis	0.05740	18.08

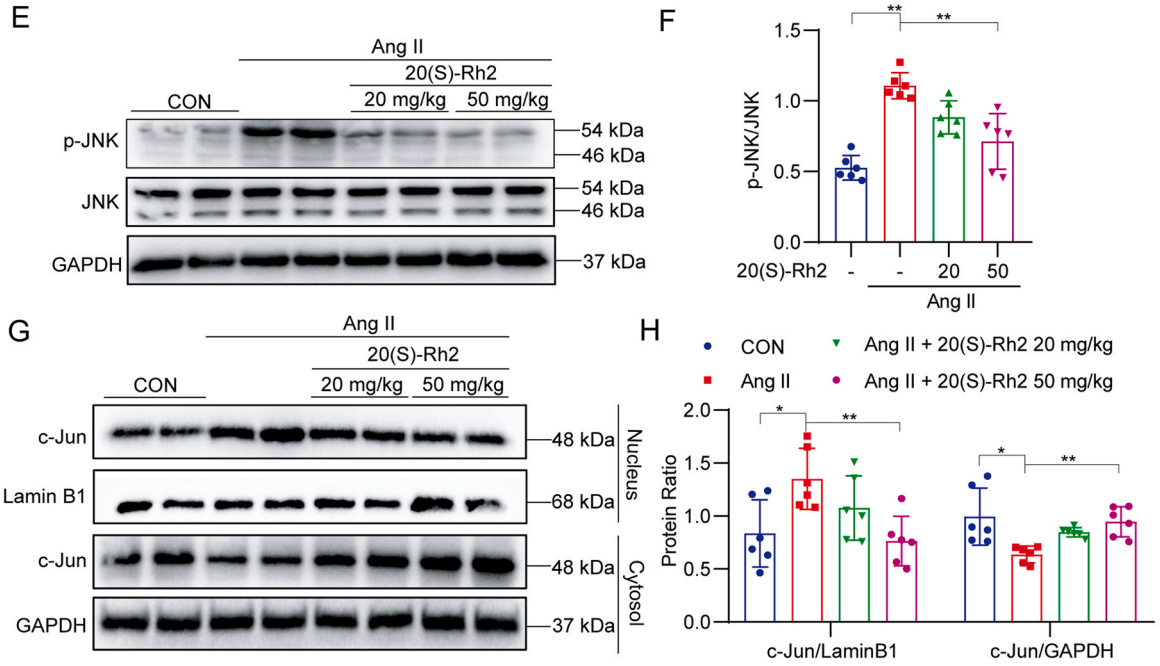

Fig. 3. The 20(S)-Rh2 cardioprotective effect is linked to JNK/AP-1 inhibition. (A–B) Volcano map depicting differentially expressed genes across Ang-II treated and control mice and (A) between the Ang-II and 20(S)-Rh2 + Ang-II mice (B); the red, blue, and gray colors depict the upregulated, downregulated, and no difference genes, respectively. (C) Venn diagram indicating the upregulated genes in the Ang-II treated vs. the control and 20(S)-Rh2 pretreatment + Ang-II groups. (D) Bio Planet 2019 pathway data list, followed by intersecting genes expression assessment in plane C. (E) Heart tissues' p-JNK and JNK western blot results. GAPDH was utilized as endogenous control. (F) Proteins' quantitative blot intensity data was assessed via ImageJ in plane E. (G) Nuclear and cytosolic levels of c-Jun in Ang-II treated mice heart lysates were assessed by immunoblotting. (H) Proteins' quantitative blot intensity data was assessed via ImageJ in plane G. Datasets reflected Mean ± SEM; n = 6; * = $p < 0.05$, ** = $p < 0.01$, two-tailed Student's *t*-test.

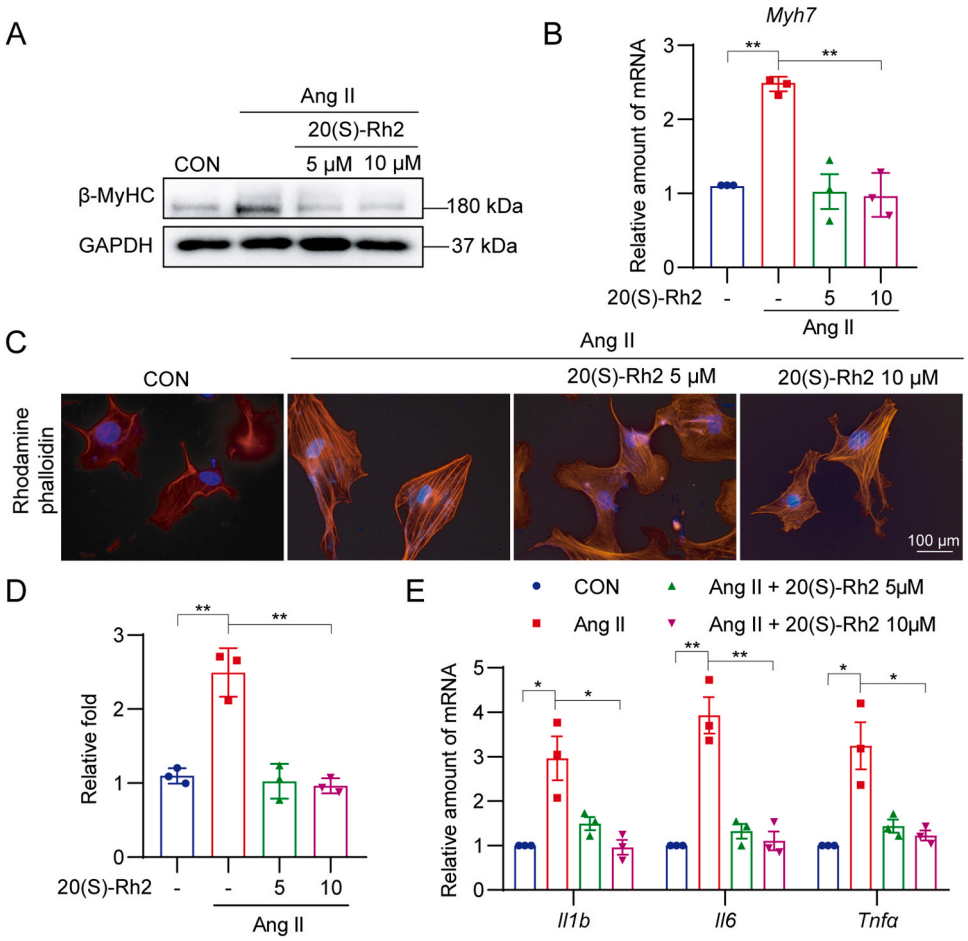

Fig. 4. 20(S)-Rh2 inhibits Ang-II-mediated fibrosis, inflammation, and hypertrophy in NRVMs. NRVMs were pretreated for 1 h with 20(S)-Rh2 (5 or 10 μM) and then for 8 or 24 h with Ang-II (1 μM). (A) β-MyHC levels in NRVMs as determined by western blot analysis. GAPDH was utilized as endogenous control. (B) *Myh7* mRNA level in NRVMs was assessed by RT-qPCR. (C) Images of Tetramethyl rhodamine phalloidin (red) stained NRVMs indicating the influence of 20(S)-Rh2 on Ang-II-triggered hypertrophic responses. DAPI was utilized as the counterstain (blue) (scale bar = 100 μm). (D) Quantification of NRVMs size increment induced by Ang-II and 20(S)-Rh2s' impact on this increase. At least 100 cells (4 samples/group) were calculated from various visual fields. (E) *Il1b*, *Tnfa*, and *Il6* mRNA levels in NRVMs were assessed by RT-qPCR. Datasets reflected Mean ± SEM; n = 3; * = $p < 0.05$, ** = $p < 0.01$, two-tailed Student's *t*-test.

damages, and 20(S)-Rh2s' pharmacological impacts were alleviated with MAPK suppression by commercial small-molecule inhibitors. These data indicate that 20(S)-Rh2 is an efficient drug against HHF, and AP-1 and JNK are potential targets for reducing pathological remodeling of the cardiac system and its inflammation. The visual abstract graphically depicts the primary findings of this investigation.

Controlling blood pressure effectively avoids hypertensive heart remodeling, a substantial reason for global CV mortality. However, effective medicines that inhibit cardiac fibrosis and enlargement are lacking. The pig model demonstrated that dapagliflozin reduces left ventricular concentric hypertrophy progression by inhibiting inflammatory response [25]. Here, it was observed that 20(S)-Rh2 might alleviate the cardiac pathologic alterations without affecting blood pressure. 20(S)-Rh2 possesses anti-inflammatory activity protecting murine hearts from pathologic re-modeling due to cardiac hypertrophy/fibrosis. Recent research demonstrated few ginsenosides, including Rb1, Rg3, and Rg2 have been shown to inhibit Ang-II-mediated myocardial fibrosis/hypertrophy [26–28]. Therefore, ginsenosides may furnish treatment for Ang-II-induced heart failure.

Ginseng is a common herb with various medicinal effects. One of its primary active components, 20(S)-Rh2, has been shown to have powerful pharmacological properties in many cancer models, including cardio- and hepato-protection [29–32]. Recent research indicates 20 (S)-Rh2 reduces tumor development by blocking the AXL, MAPK, and AKT pathways; however, the exact targets are unclear [18,33]. Per our knowledge, this is the 1st investigation to observe that 20(S)-Rh2 markedly inhibits Ang-II-mediated cardiac remodeling and dysfunction via its anti-inflammatory effect.

The JNK/MAPK signaling pathway was observed to link with this effect, as indicated by RNA sequencing. The JNK signaling pathway is linked with various disorders, including cancers and neurological, immunological, and inflammatory disorders [34]. Furthermore, JNK kinases are also associated with different cardiomyocyte propagation and fibrosis pathways. In end-stage heart failure, JNK is observed to be activated [35], and the levels of its upstream activator MLK expression are increased [36]. This investigation revealed that Ang-II increased the activation of phosphorylated JNK within cardiac tissue and propagated cardiomyocytes, heavily reversed through 20(S)-Rh2. Furthermore, JNK suppression through SP600125 reversed 20(S)-Rh2's impact upon cardiomyocytes, suggesting JNK modulates 20(S)-Rh2s' cardioprotective and anti-inflammatory properties.

20(S)-Rh2s' putative transcriptional component associated to cardioprotective functions were concentrated. AP-1 reflects canonical JNK downstream transcriptional factor. After phosphorylation by PI3K/Akt and JNK, cytoplasmic AP-1 (c-Jun) transfers into nuclei to modulate target gene expression [37,38]. AP-1 directly modulated cardiac fibrosis-linked genes (*Tgfb1* and *Col1*) exhibiting mortal phenotype [39]. Transient AP-1 activation increases cardiomyocyte propagation in response to various stimuli, such as adrenergic and fatty acid signals [40]. Ang-II promoted AP-1 nuclear translocation in wild-type mice,

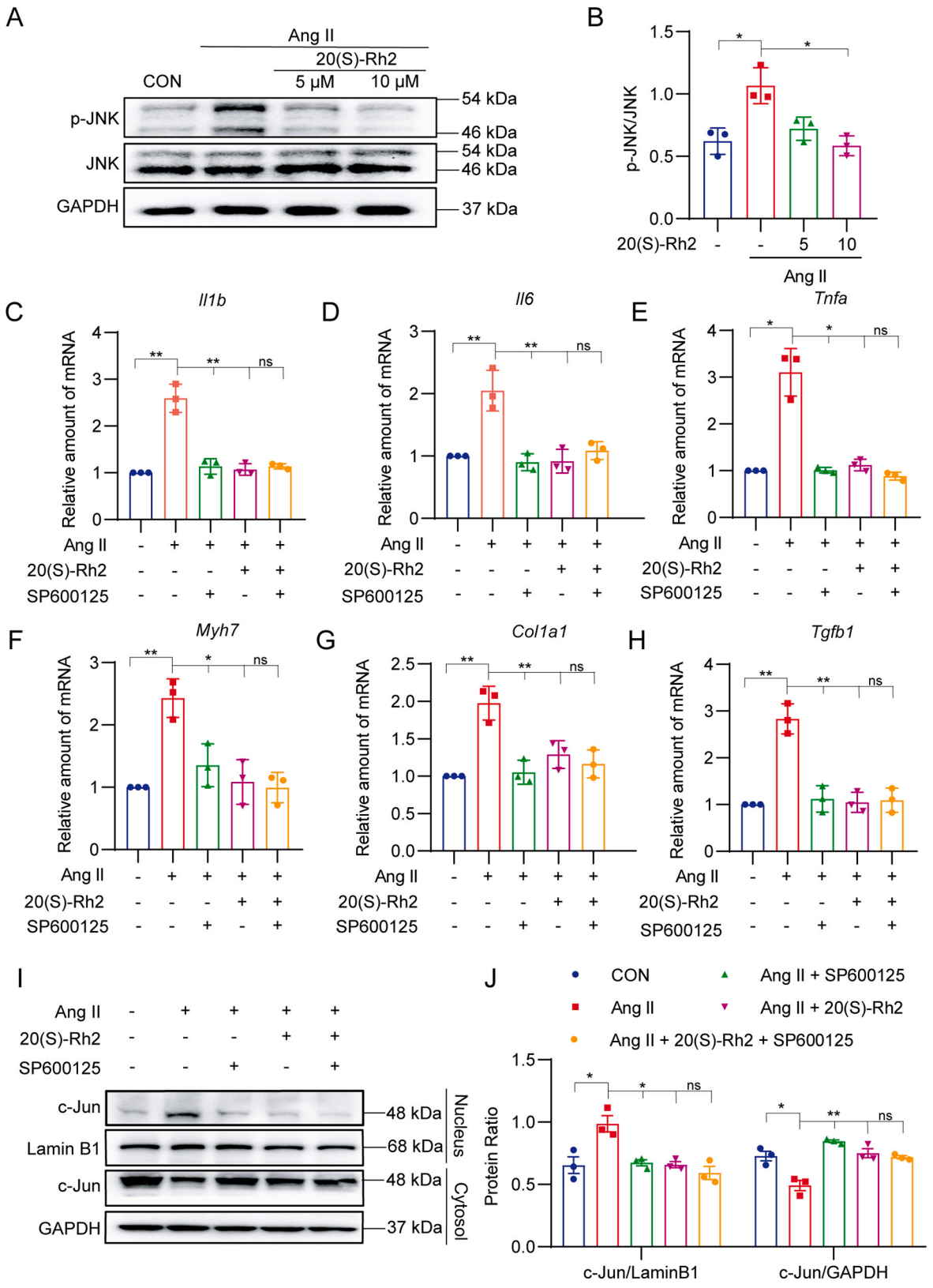

Fig. 5. 20(S)-Rh2 protects cardiomyocytes by inhibiting JNK/AP-1 activation. NRVMs were pretreated with 20(S)-Rh2 with or without SP600125. (A) Western blot data of p-JNK and JNK in NRVMs. GAPDH was utilized as endogenous control. (B) Proteins' quantitative blot intensity data was assessed via ImageJ in plane A. (C–E) RT-qPCR indicated the *Il1b*, *Il6*, and *Tnfα* mRNA levels in NRVMs. (F–H) RT-qPCR indicated the *MyH7*, *Col1a1*, and *Tgfb1* mRNA levels in NRVMs. (I) The nuclear and cytosolic c-Jun levels were elucidated by immunoblotting. GAPDH and Lamin B were utilized as endogenous control. (J) Proteins' quantitative blot intensity data was assessed via ImageJ in the plane I. Datasets reflected Mean ± SEM; n = 3; ns = not significant; * = $p < 0.05$, ** = $p < 0.01$, two-tailed Student's *t*-test.

counteracted by 20(S)-Rh2 in a dose-reliant pattern consistent with those observed in propagated cardiomyocytes. Ang-II-mediated AP-1 overexpression was markedly reduced through JNK thwarting with either SP600125 or 20(S)-Rh2. Suggesting that Ang-II stimulates JNK/AP-1 axis, causing cardiac fibrosis/hypertrophy.

In addition to the JNK/AP-1 signaling pathway, 20 (S) - Rh2 may also protect the heart by regulating other signaling pathways. For example, ginsenoside Rh2 inhibits heart fibrosis in type 1 diabetic rats by activating PPARδ-STAT3 [10]. Recently, a large number of studies have confirmed that the etiology of HHF is related to these pathways. More research is required to assess the relative importance of each pathway in 20(S)-Rh2s' pharmacological effects, the direct 20(S)-Rh2 interaction with JNK, and 20(S)-Rh2 molecular targets which suppress JNK activation.

In summary, suppressing JNK-stimulated cardiac inflammation by 20(S)-Rh2 safeguards Ang-II-mediated hypertension in mice's hearts, indicating that 20(S)-Rh2 is an efficient treatment avenue for HHF.

Declaration of Competing Interest

The authors declare that they have no known competing financial interests or personal relationships that could have appeared to influence the work reported in this paper.

Acknowledgment

This work is supported by the National Natural Science Foundation of China (82000793 to W.L. and 21961142009 to G.L.).

Author contributions

Guang Liang and Mengyang Wang contributed the central idea, analysed most of the data, and wrote the initial draft of the paper. To refine these ideas, other authors conducted additional analysis. All authors have contributed to the completion of this article. All authors read and approved the final manuscript.

Appendix A. Supporting information

Supplementary data associated with this article can be found in the online version at doi:10.1016/j.biopha.2023.115880.

References

[1] A.E. Dikalova, A. Pandey, L. Xiao, L. Arslanbaeva, T. Sidorova, M.G. Lopez, F. Tt Billings, E. Verdin, J. Auwerx, D.G. Harrison, S.I. Dikalov, Mitochondrial deacetylase Sirt3 reduces vascular dysfunction and hypertension while Sirt3 depletion in essential hypertension is linked to vascular inflammation and oxidative stress, Circ. Res. 126 (4) (2020) 439–452.
[2] V. Sepúlveda-Fragoso, B. Alexandre-Santos, A. Salles, A. Proença, A. de Paula Alves, M. Vázquez-Carrera, A. Nóbrega, E. Frantz, D. Magliano, Crosstalk between the renin-angiotensin system and the endoplasmic reticulum stress in the cardiovascular system: lessons learned so far, Life Sci. 284 (2021), 119919.
[3] A. Montezano, A. Nguyen Dinh Cat, F. Rios, R. Touyz, Angiotensin II and vascular injury, Curr. Hypertens. Rep. 16 (6) (2014), 431.
[4] J. Wu, E. Dong, Y. Zhang, H. Xiao, The role of the inflammasome in heart failure, Front. Physiol. 12 (2021), 709703.
[5] L. Arendse, A. Danser, M. Poglitsch, R. Touyz, J. Burnett, C. Llorens-Cortes, M. Ehlers, E. Sturrock, Novel therapeutic approaches targeting the renin-angiotensin system and associated peptides in hypertension and heart failure, Pharmacol. Rev. 71 (4) (2019) 539–570.
[6] Y. Wang, J. Dong, P. Liu, C. Lau, Z. Gao, D. Zhou, J. Tang, C. Ng, Y. Huang, Ginsenoside Rb3 attenuates oxidative stress and preserves endothelial function in renal arteries from hypertensive rats, Br. J. Pharmacol. 171 (13) (2014) 3171–3181.
[7] J. Zhang, M. Liu, M. Huang, M. Chen, D. Zhang, L. Luo, G. Ye, L. Deng, Y. Peng, X. Wu, G. Liu, W. Ye, D. Zhang, Ginsenoside F1 promotes angiogenesis by activating the IGF-1/IGF1R pathway, Pharmacol. Res. 144 (2019) 292–305.
[8] R. Alolga, G. Nuer-Allornuvor, E. Kuugbee, X. Yin, G. Ma, Ginsenoside Rg1 and the control of inflammation implications for the therapy of type 2 diabetes: a review of scientific findings and call for further research, Pharmacol. Res. 152 (2020), 104630.
[9] Y. Zhu, C. Zhu, H. Yang, J. Deng, D. Fan, Protective effect of ginsenoside Rg5 against kidney injury via inhibition of NLRP3 inflammasome activation and the MAPK signaling pathway in high-fat diet/streptozotocin-induced diabetic mice, Pharmacol. Res. 155 (2020), 104746.
[10] S. Lo, C. Hsu, H. Niu, C. Niu, J. Cheng, Z. Chen, Ginsenoside Rh2 improves cardiac fibrosis via PPARδ-STAT3 signaling in Type 1-Like diabetic rats, Int. J. Mol. Sci. 18 (7) (2017).
[11] X. Chen, T. Xu, X. Lv, J. Zhang, S. Liu, Ginsenoside Rh2 alleviates ulcerative colitis by regulating the STAT3/miR-214 signaling pathway, J. Ethnopharmacol. 274 (2021), 113997.
[12] H. Zhang, S. Park, H. Huang, E. Kim, J. Yi, S. Choi, Z. Ryoo, M. Kim, Anticancer effects and potential mechanisms of ginsenoside Rh2 in various cancer types (Review), Oncol. Rep. 45 (4) (2021).
[13] J. Wang, H. Wang, X. Mou, M. Luan, X. Zhang, X. He, F. Zhao, Q. Meng, The advances on the protective effects of ginsenosides on myocardial ischemia and ischemia-reperfusion injury, Mini Rev. Med. Chem. 20 (16) (2020) 1610–1618.
[14] X. Li, S. Chu, M. Lin, Y. Gao, Y. Liu, S. Yang, X. Zhou, Y. Zhang, Y. Hu, H. Wang, N. Chen, Anticancer property of ginsenoside Rh2 from ginseng, Eur. J. Med. Chem. 203 (2020), 112627.
[15] J. Hou, Y. Yun, C. Cui, S. Kim, Ginsenoside Rh2 mitigates doxorubicin-induced cardiotoxicity by inhibiting apoptotic and inflammatory damage and weakening pathological remodelling in breast cancer-bearing mice, Cell Prolif. 55 (6) (2022), e13246.
[16] S. Ye, W. Luo, Z.A. Khan, G. Wu, L. Xuan, P. Shan, K. Lin, T. Chen, J. Wang, X. Hu, S. Wang, W. Huang, G. Liang, Celastrol attenuates angiotensin II-induced cardiac remodeling by targeting STAT3, Circ. Res. 126 (8) (2020) 1007–1023.
[17] L. Wang, Y.L. Li, C.C. Zhang, W. Cui, X. Wang, Y. Xia, J. Du, H.H. Li, Inhibition of Toll-like receptor 2 reduces cardiac fibrosis by attenuating macrophage-mediated inflammation, Cardiovasc. Res. 101 (3) (2014) 383–392.
[18] H. Zhang, J. Yi, H. Huang, S. Park, W. Kwon, E. Kim, S. Jang, S. Kim, S. Choi, D. Yoon, S. Kim, K. Liu, Z. Dong, Z. Ryoo, M. Kim, 20 (S)-ginsenoside Rh2 inhibits colorectal cancer cell growth by suppressing the Axl signaling pathway in vitro and in vivo, J. Ginseng Res. 46 (3) (2022) 396–407.
[19] X. Chen, F. Qian, Y. Wang, Y. Liu, Y. Sun, W. Zha, K. Hao, F. Zhou, G. Wang, J. Zhang, Ginsenoside 20(S)-Rh2 promotes cellular pharmacokinetics and intracellular antibacterial activity of levofloxacin against Staphylococcus aureus through drug efflux inhibition and subcellular stabilization, Acta Pharmacol. Sin. 42 (11) (2021) 1930–1941.
[20] S. Alam, Q. Liu, S. Liu, Y. Liu, Y. Zhang, X. Yang, G. Liu, K. Fan, J. Ma, Up-regulated cathepsin C induces macrophage M1 polarization through FAK-triggered p38 MAPK/NF-κB pathway, Exp. Cell Res. 382 (2) (2019), 111472.
[21] S. Craige, K. Chen, R. Blanton, J. Keaney, S. Kant, JNK and cardiometabolic dysfunction, Biosci. Rep. 39 (7) (2019).
[22] J. Morgan, T. Curran, Proto-oncogene transcription factors and epilepsy, Trends Pharmacol. Sci. 12 (9) (1991) 343–349.
[23] A. Papavassiliou, A. Musti, The multifaceted output of c-Jun biological activity: focus at the junction of CD8 T cell activation and exhaustion, Cells 9 (11) (2020).
[24] M. Kappelmann, A. Bosserhoff, S. Kuphal, AP-1/c-Jun transcription factors: regulation and function in malignant melanoma, Eur. J. Cell Biol. 93 (2014) 76–81.
[25] N. Zhang, B. Feng, X. Ma, K. Sun, G. Xu, Y. Zhou, Dapagliflozin improves left ventricular remodeling and aorta sympathetic tone in a pig model of heart failure with preserved ejection fraction, Cardiovasc. Diabetol. 18 (1) (2019), 107.
[26] B. Ren, J. Feng, N. Yang, Y. Guo, C. Chen, Q. Qin, Ginsenoside Rg3 attenuates angiotensin II-induced myocardial hypertrophy through repressing NLRP3 inflammasome and oxidative stress via modulating SIRT1/NF-κB pathway, Int. Immunopharmacol. 98 (2021), 107841.
[27] S. Wang, Y. Cui, M. Xiong, M. Li, P. Wang, J. Cui, X. Du, Y. Chen, T. Zhang, Dual activity of ginsenoside Rb1 in hypertrophic cardiomyocytes and activated macrophages: implications for the therapeutic intervention of cardiac hypertrophy, J. Inflamm. Res. 14 (2021) 1789–1806.
[28] X. Zheng, S. Wang, X. Zou, Y. Jing, R. Yang, S. Li, F. Wang, Ginsenoside Rb1 improves cardiac function and remodeling in heart failure, Exp. Anim. 66 (3) (2017) 217–228.
[29] J. Yang, D. Yuan, T. Xing, H. Su, S. Zhang, J. Wen, Q. Bai, D. Dang, Ginsenoside Rh2 inhibiting HCT116 colon cancer cell proliferation through blocking PDZ-binding kinase/T-LAK cell-originated protein kinase, J. Ginseng Res. 40 (4) (2016) 400–408.
[30] T. Tong-Lin Wu, Y. Tong, I. Chen, H. Niu, Y. Li, J. Cheng, Induction of apoptosis in prostate cancer by ginsenoside Rh2, Oncotarget 9 (13) (2018) 11109–11118.
[31] G. Ge, Y. Yan, H. Cai, Ginsenoside Rh2 inhibited proliferation by inducing ROS mediated ER stress dependent apoptosis in lung cancer cells, Biol. Pharm. Bull. 40 (12) (2017) 2117–2124.
[32] H. Wang, P. Yu, H. Gou, J. Zhang, M. Zhu, Z. Wang, J. Tian, Y. Jiang, F. Fu, Cardioprotective effects of 20(S)-Ginsenoside Rh2 against doxorubicin-induced cardiotoxicity in vitro and in vivo, Evid. -Based Complement. Altern. Med.: eCAM 2012 (2012), 506214.
[33] X. Shi, J. Yang, G. Wei, Ginsenoside 20(S)-Rh2 exerts anti-cancer activity through the Akt/GSK3β signaling pathway in human cervical cancer cells, Mol. Med. Rep. 17 (3) (2018) 4811–4816.
[34] K. Sabapathy, Role of the JNK pathway in human diseases, Prog. Mol. Biol. Transl. Sci. 106 (2012) 145–169.
[35] S. Cook, P. Sugden, A. Clerk, Activation of c-Jun N-terminal kinases and p38-mitogen-activated protein kinases in human heart failure secondary to ischaemic heart disease, J. Mol. Cell. Cardiol. 31 (8) (1999) 1429–1434.
[36] T. Calamaras, R. Baumgartner, M. Aronovitz, A. McLaughlin, K. Tam, D. Richards, C. Cooper, N. Li, W. Baur, X. Qiao, G. Wang, R. Davis, N. Kapur, R. Karas,

R. Blanton, Mixed lineage kinase-3 prevents cardiac dysfunction and structural remodeling with pressure overload, Am. J. Physiol. Heart Circ. Physiol. 316 (1) (2019) H145–H159.
[37] W. Dong, Y. Li, M. Gao, M. Hu, X. Li, S. Mai, N. Guo, S. Yuan, L. Song, IKKα contributes to UVB-induced VEGF expression by regulating AP-1 transactivation, Nucleic Acids Res. 40 (7) (2012) 2940–2955.
[38] H. Menden, S. Welak, S. Cossette, R. Ramchandran, V. Sampath, Lipopolysaccharide (LPS)-mediated angiopoietin-2-dependent autocrine angiogenesis is regulated by NADPH oxidase 2 (Nox2) in human pulmonary microvascular endothelial cells, J. Biol. Chem. 290 (9) (2015) 5449–5461.
[39] M. Karin, The regulation of AP-1 activity by mitogen-activated protein kinases, Philos. Trans. R. Soc. Lond. Ser. B, Biol. Sci. 351 (1336) (1996) 127–134.
[40] H. Zhang, L. Pei, Z. Ouyang, H. Wang, X. Chen, K. Jiang, S. Huang, R. Jiang, Y. Xiang, K. Wei, AP-1 activation mediates postnatal cardiomyocyte maturation, Cardiovasc. Res. (2022).